TEMPORAL IMAGING AND SUPER-RESOLVED SPECTROSCOPY WITH A QUANTUM MEMORY

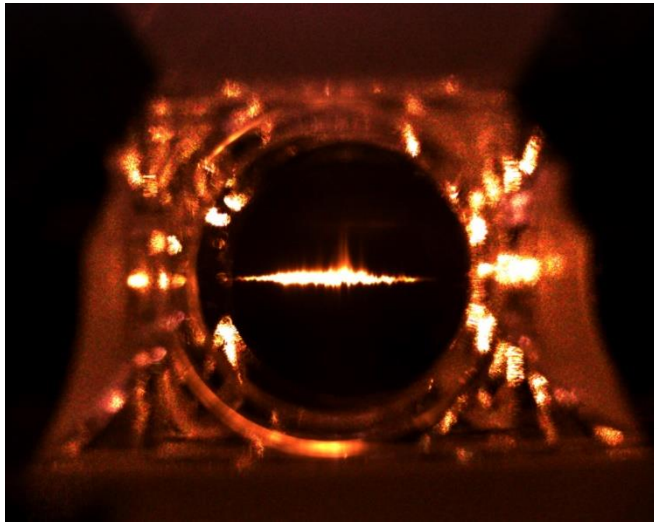

Michał Parniak
Mateusz Mazelanik, Adam Leszczyński,
Michał Lipka, Wojciech Wasilewski
Konrad Banaszek
Centre for Quantum Optical Technologies
University of Warsaw
qot.uw.edu.pl

European Funds Smart Growth
Republic of Poland
FNP Foundation for Polish Science
European Union European Regional Development Fund
Office of Naval Research Science & Technology

SPIE Optics+Photonics

U. of Warsaw

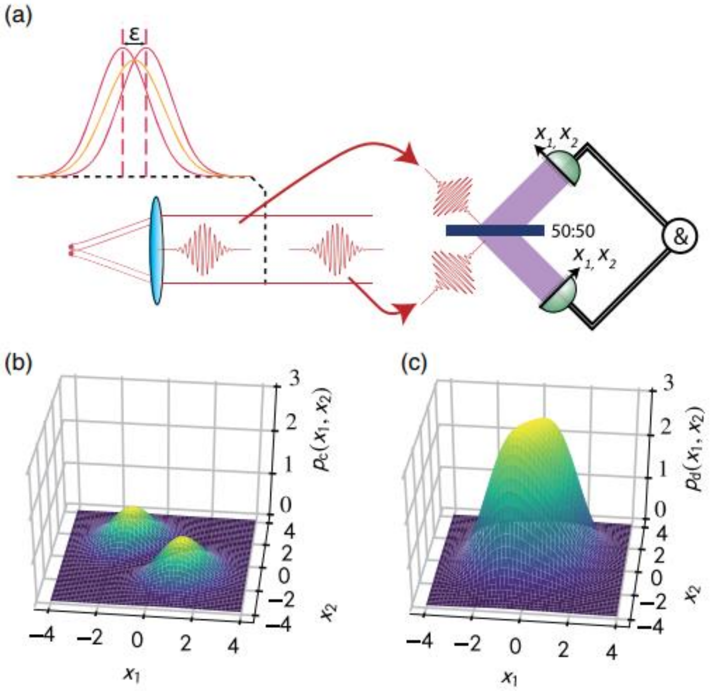

PHYSICAL REVIEW LETTERS 121, 250503 (2018)
With Konrad Banaszek and Rafał Demkowicz-Dobrzański

NBI/Copenhagen

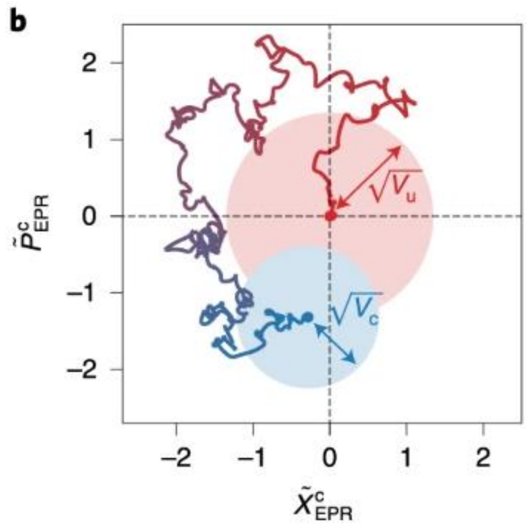

Nature Physics **17**, 228–233 (2021)
With Eugene S. Polzik

Imaging resolution - Rayleigh Criterion

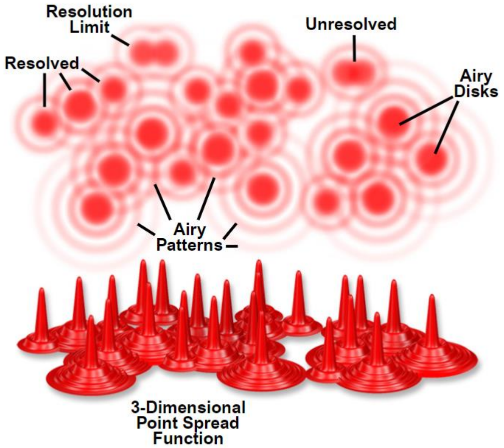

$$\theta = 1{\cdot}2197 \frac{\lambda}{2R}$$

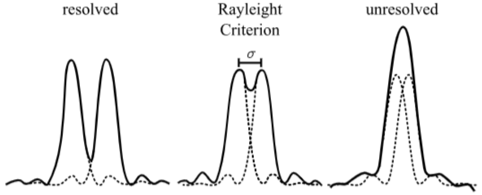

$$\sigma = \frac{0.61\lambda}{\mu \sin\gamma} = \frac{0.61\lambda}{NA}$$

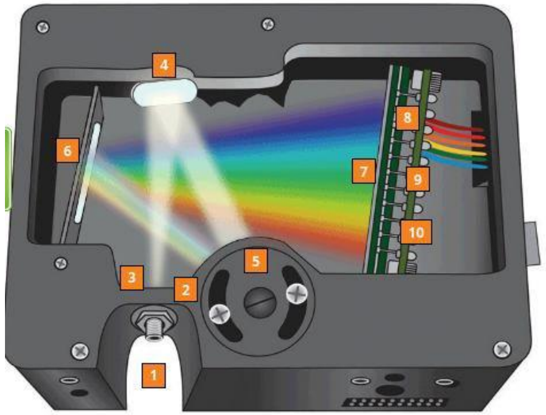

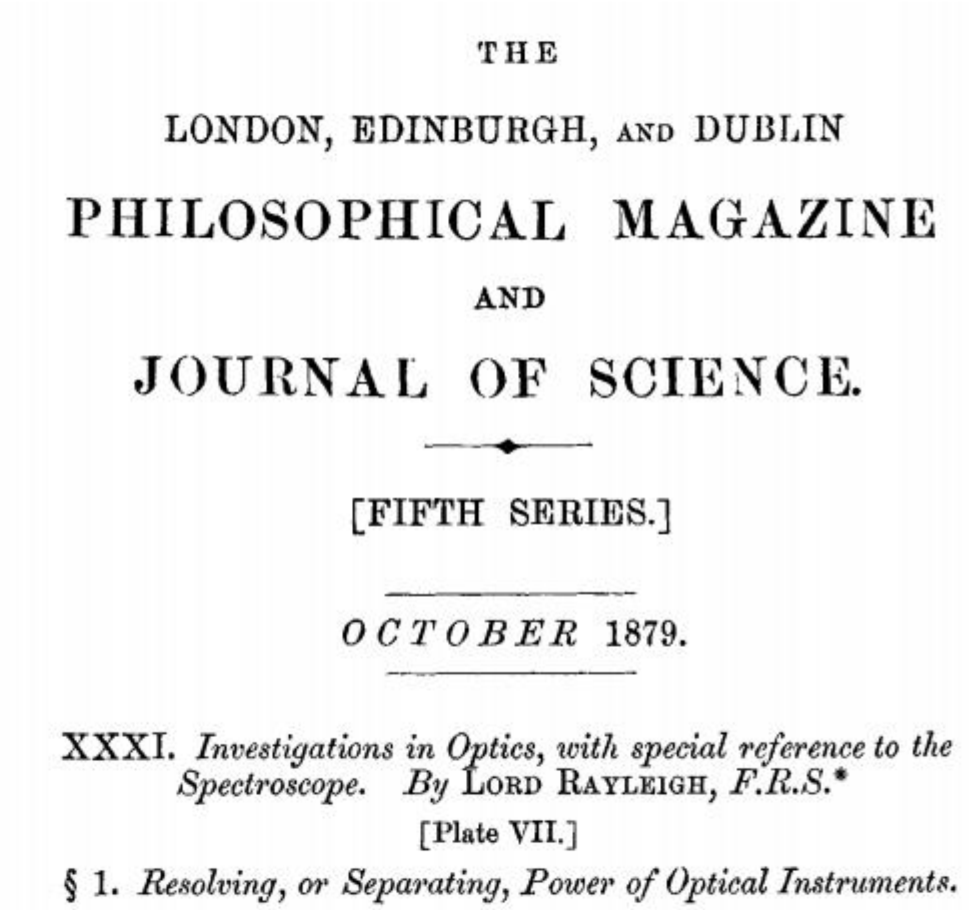

THE

LONDON, EDINBURGH, AND DUBLIN

PHILOSOPHICAL MAGAZINE

AND

JOURNAL OF SCIENCE.

[FIFTH SERIES.]

OCTOBER 1879.

XXXI. *Investigations in Optics, with special reference to the Spectroscope.* By LORD RAYLEIGH, *F.R.S.**

[Plate VII.]

§ 1. *Resolving, or Separating, Power of Optical Instruments.*

microscopyu.com oceaninsight.com

Rayleigh Limit

Two point sources:

$$|u(x+\varepsilon/2)|^2 + |u(x-\varepsilon/2)|^2$$

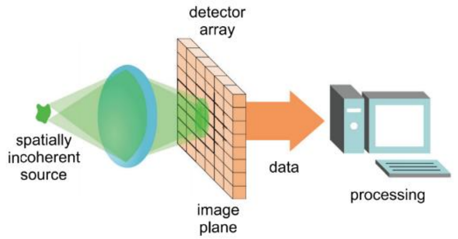

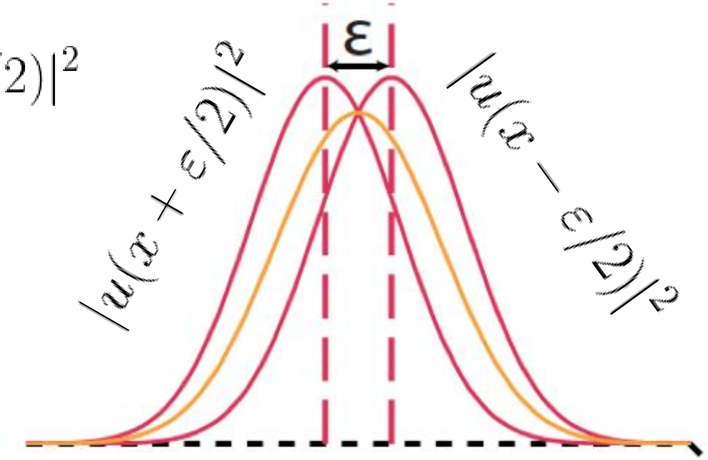

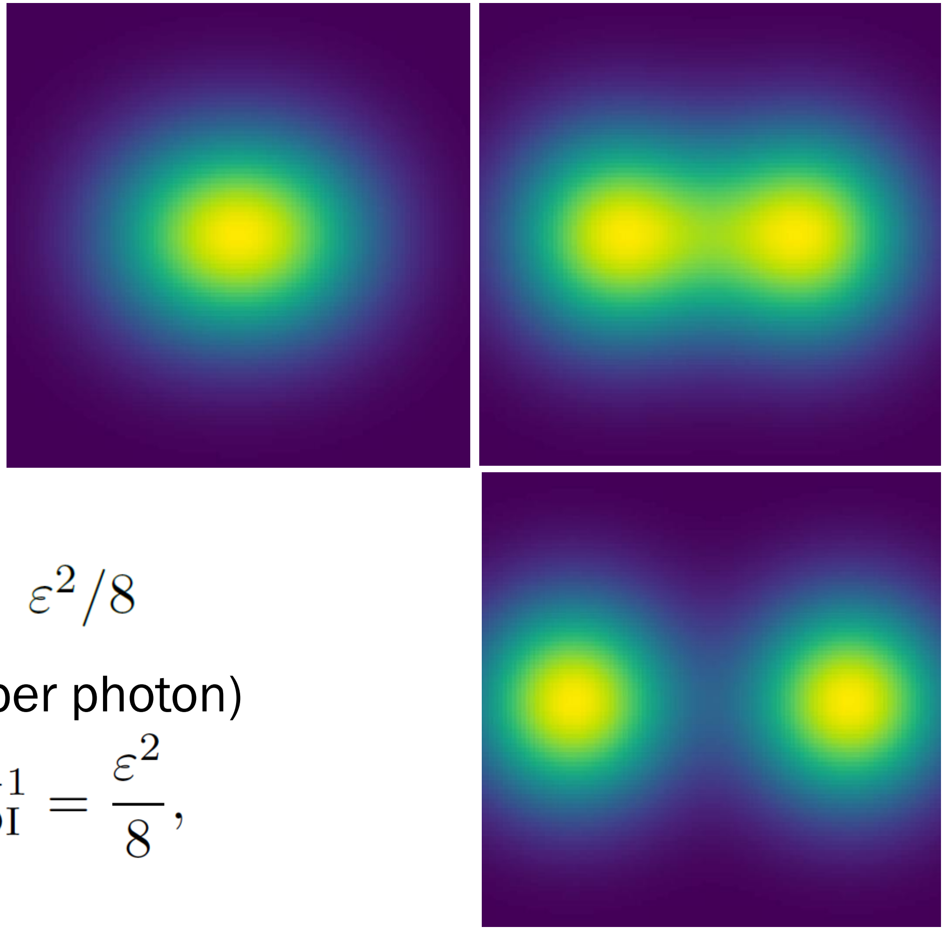

Cramér–Rao bound (CRB)

$$\Delta^2\hat{\varepsilon} \geq \frac{1}{\mathcal{F}}, \mathcal{F} = \int \frac{1}{p_\varepsilon(x)}\left(\frac{\partial}{\partial\varepsilon}p_\varepsilon(x)\right)^2 \mathrm{d}x$$

$$\mathcal{F}_{\mathrm{DI}} \approx \varepsilon^2/8$$

Precision (per photon)

$$(\Delta^2\varepsilon)^{-1}_{\mathrm{DI}} = \frac{\varepsilon^2}{8},$$

Ultimate bound

Quantum Cramer-Rao bound – optimized over all possible states and measurements
Precision = Inverse Uncertainties^2 per photons

$$\theta = (x_0, \varepsilon)$$
$$\mathrm{Cov}\theta \geq N\mathcal{F}_Q$$
$$(\Delta^2 x_0)_{\mathrm{Q}}^{-1} = 1 - \frac{\varepsilon^2}{4},$$
$$(\Delta^2 \varepsilon)_{\mathrm{Q}}^{-1} = \frac{1}{4},$$

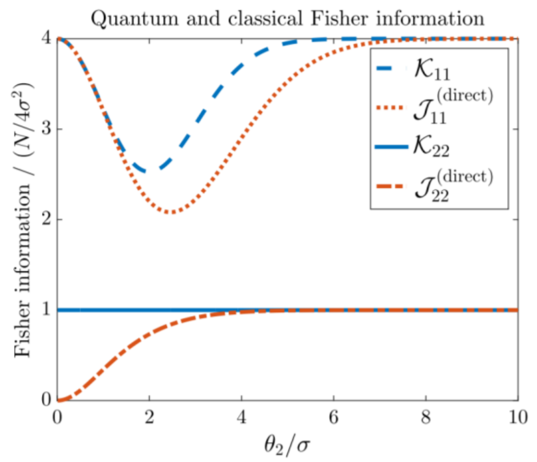

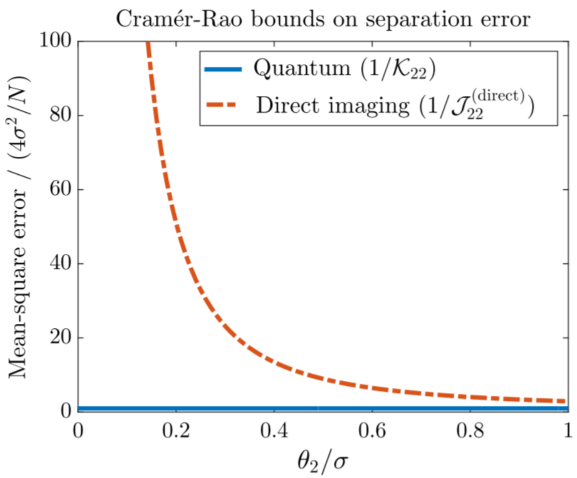

Constant precision of separation estimation – much more information available

Better measurement scheme needed!

Phys. Rev. X 6, 031033

Beating the Rayleigh Limit

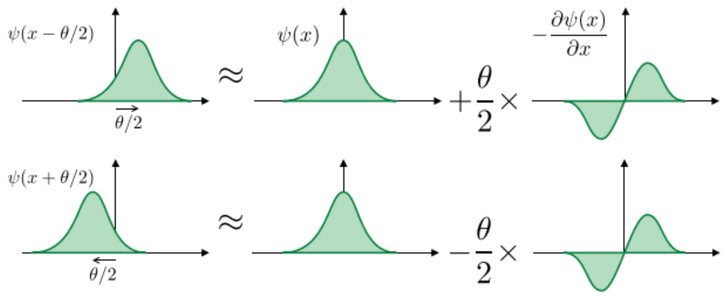

SLI
via $\mathcal{F}_{\text{SLIVER}} \approx \frac{1}{4} - \frac{\varepsilon^2}{32}$ etry)

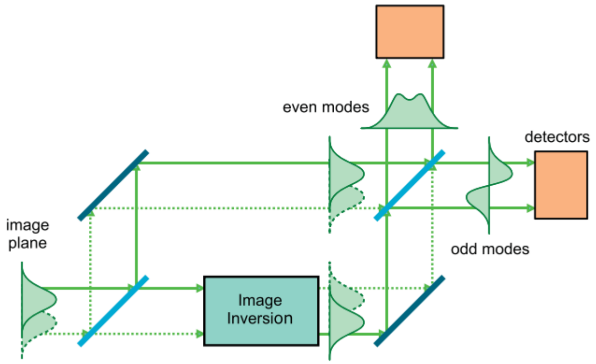

SPADE (spatial-mode demultiplexing)

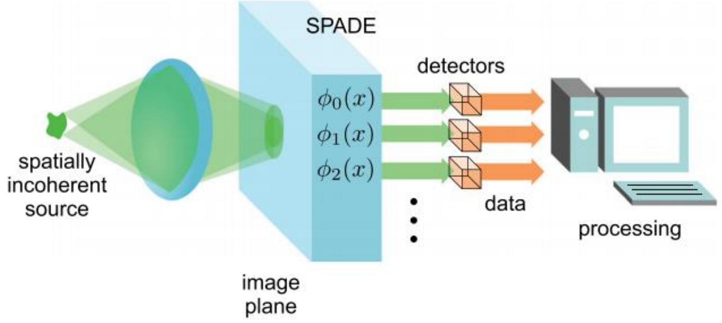

SPLICE (super-resolved position localization by inversion of coherence along an edge)

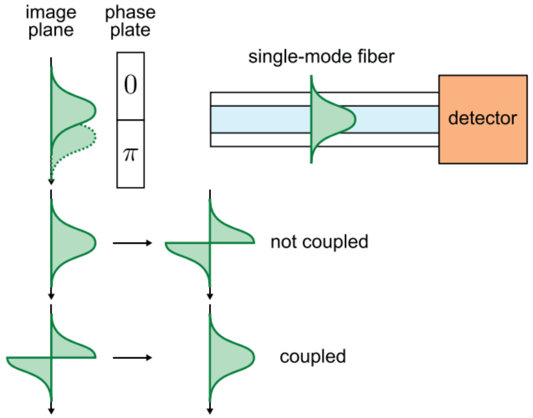

Contemporary Physics, 60:4, 279-298

Ultranarrowband optical spectroscopy

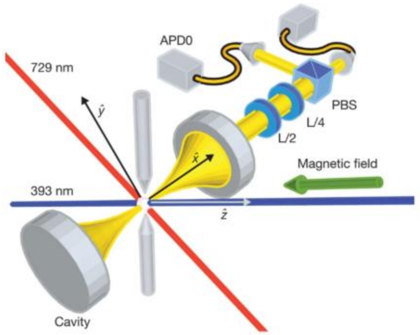

Single ions <100kHz

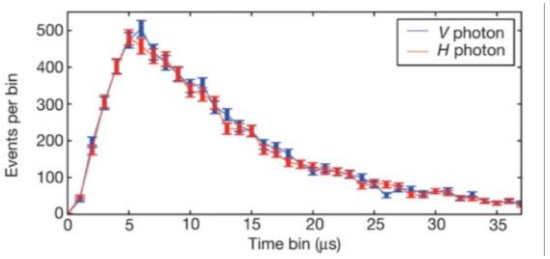

Nature 485, 482–485(2012)

Optomechanical systems
~10kHz

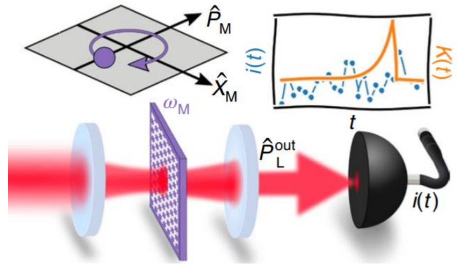

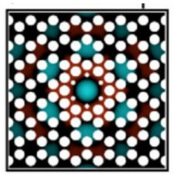

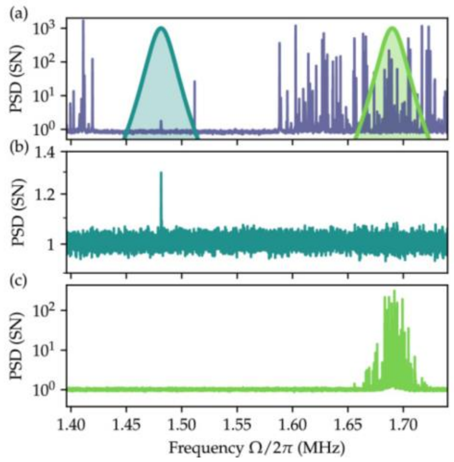

Optica 7, 718-725 (2020)

Hot and cold atoms MHz-kHz

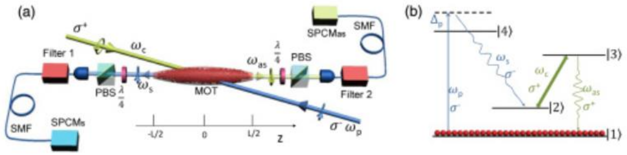

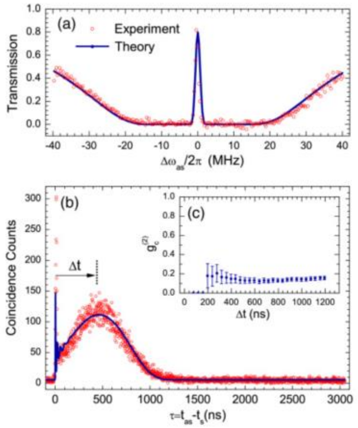

Optica 1, pp. 84-88 (2014)

System – gradient echo memory in cold rubidium-87 atoms

$T \sim 20 - 100\ \mu K$

(Not ultracold)

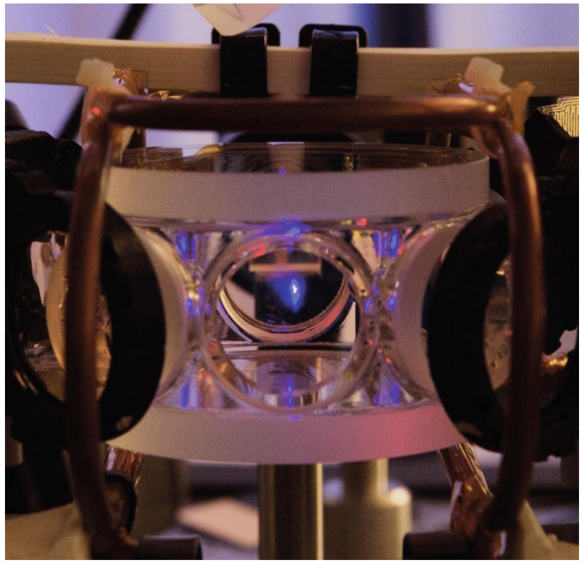

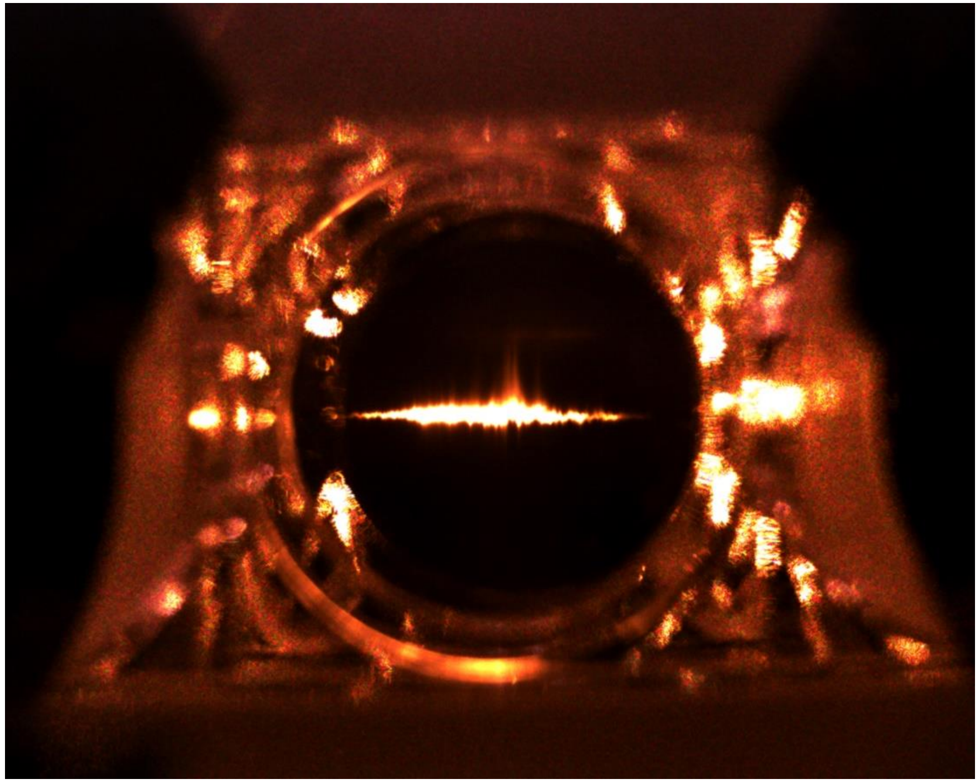

Wavevector multiplexed quantum memory (without GEM, 665 wavevector modes)

Nat. Commun **8**, 2140 (2017)

Far-field temporal imaging

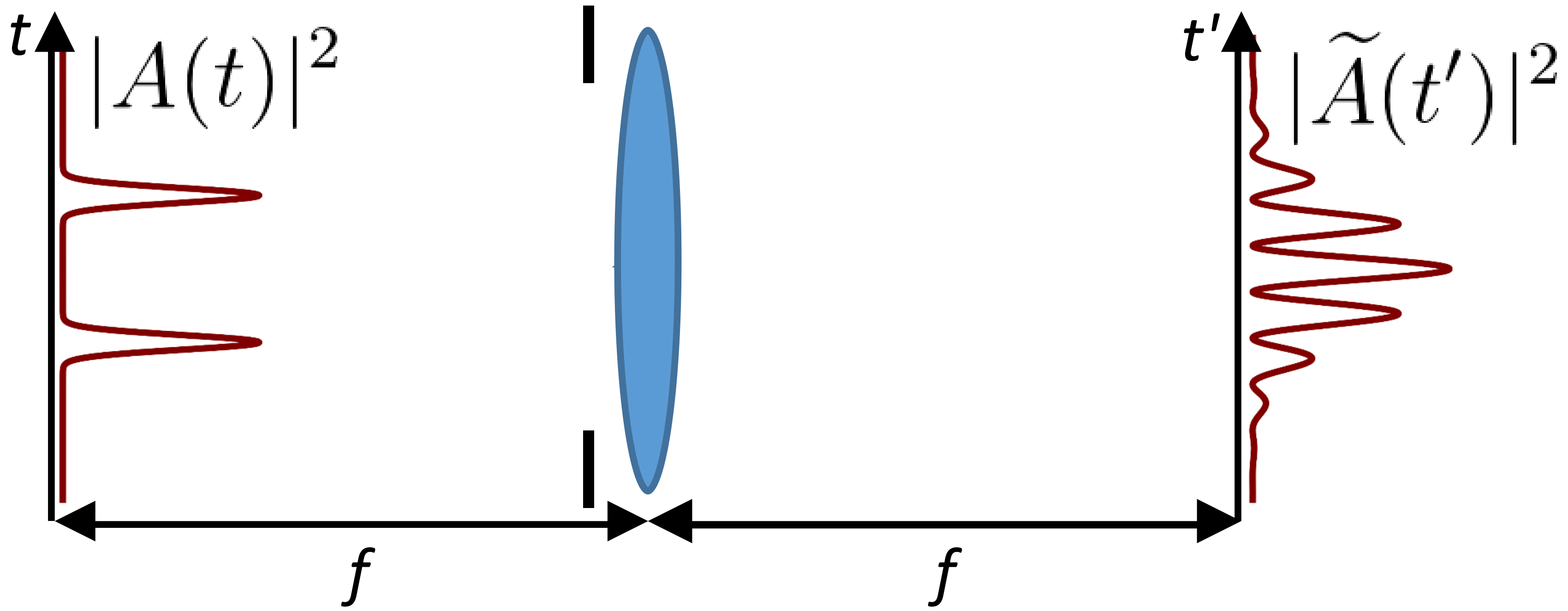

$$|\widetilde{A}(t')|^2 = |\mathcal{F}_t[A(t)](t')|^2$$

Temporal imaging

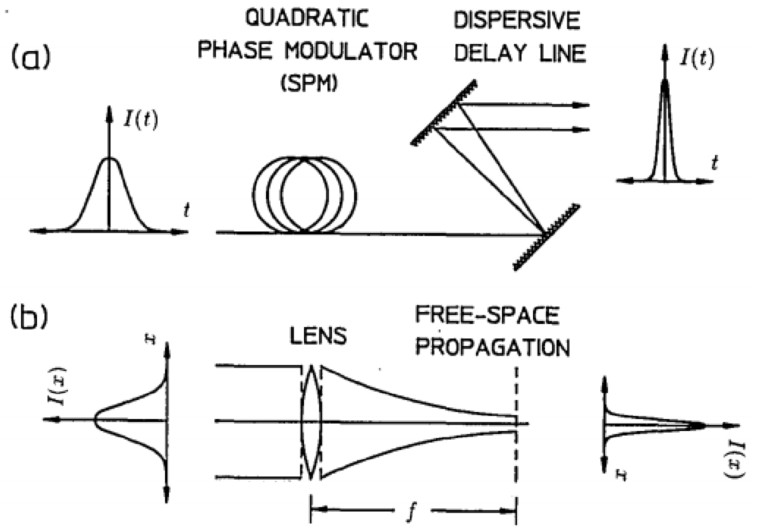

Opt. Lett. 14, 630 (1989)

- Spectral conversion
- Bandwidth manipulation
- Temporal ghost imaging
- Characterization of the time-frequency entanglement
- Manipulation of field-orthogonal temporal modes

Existing solutions are compatible with solid-state emission (high bandwith, low spectral resolution)

No solution for narrowband atomic emission

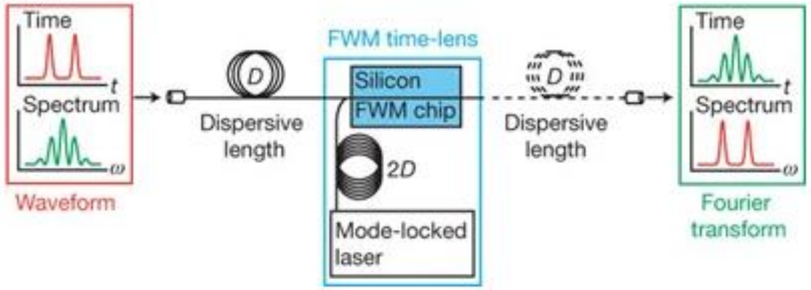

Nature 456, 81–84 (2008)

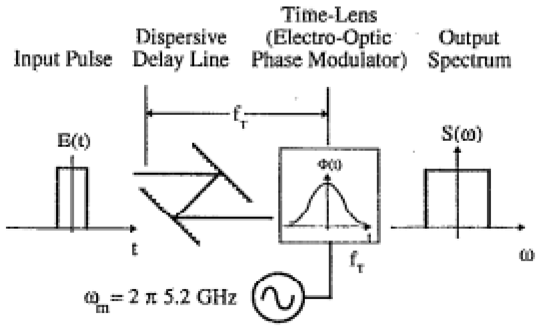

Appl. Phys. Lett. 64, 270–272 (1994)

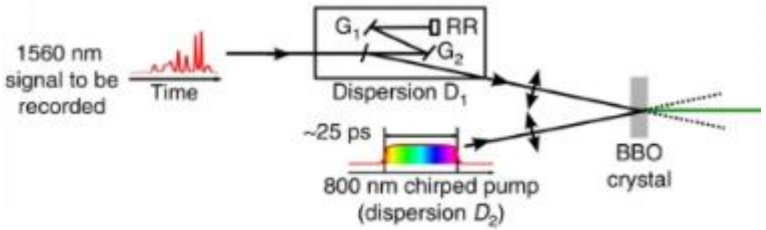

Nat. Commun. 7, 13136 (2016)

Light-atom interface

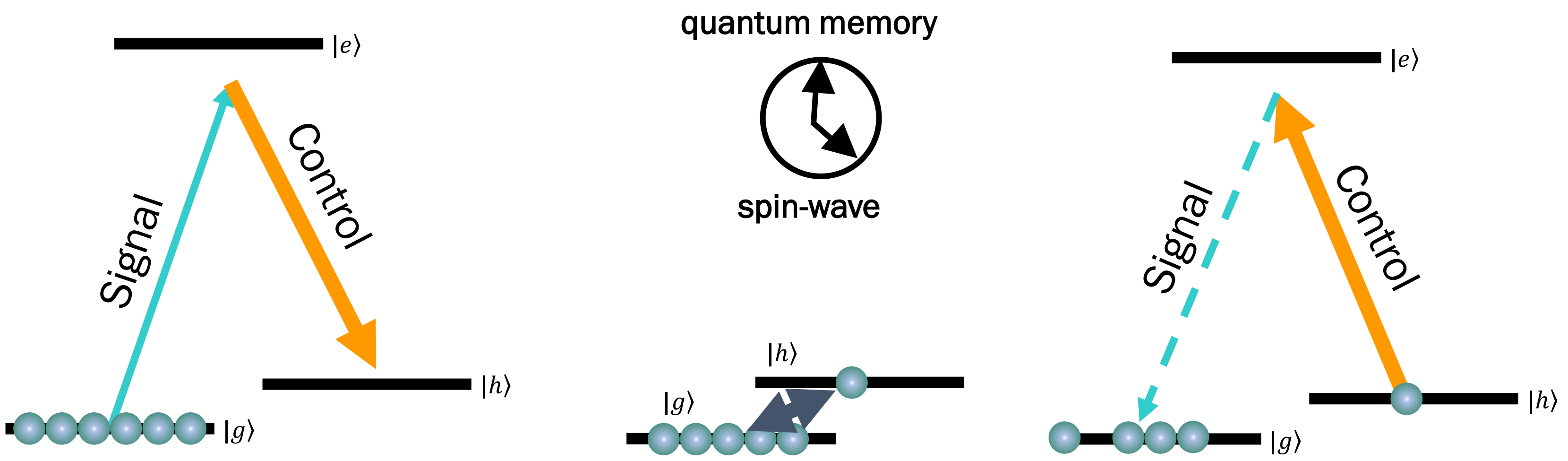

$$\hat{\rho}(\mathbf{r}) = \frac{1}{1+|\beta(\mathbf{r})|^2}\begin{pmatrix} 1 & \beta(\mathbf{r})e^{i\mathbf{K}\cdot\mathbf{r}} \\ \beta^*(\mathbf{r})e^{-i\mathbf{K}\cdot\mathbf{r}} & |\beta(\mathbf{r})|^2 \end{pmatrix}.$$

Spin wave

Gradient echo memory (GEM)

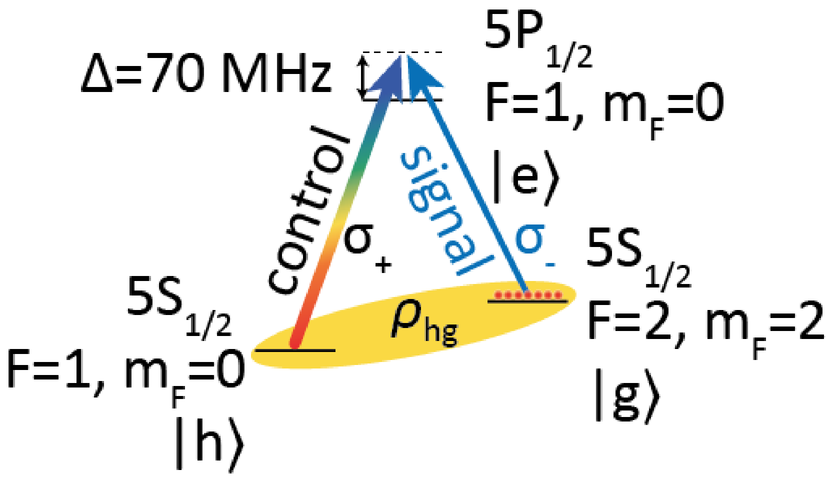

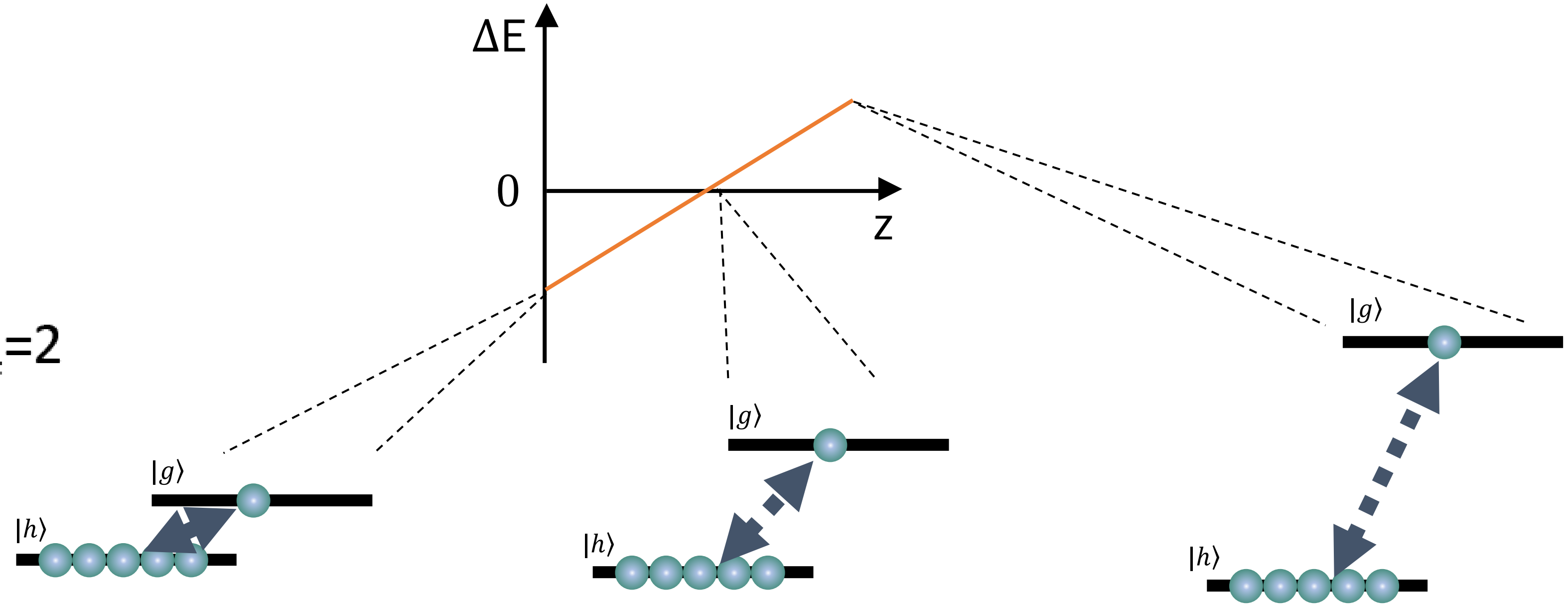

$$\frac{\partial \check{\rho}_{hg}(z,t)}{\partial t} = \frac{i}{\hbar}\frac{\Omega^*(t) d A(z,t)}{4\Delta - 2i\Gamma} - \frac{1}{2\tau}\check{\rho}_{hg}(z,t) + \boxed{i\delta_{\text{tot}}(z,t)}\check{\rho}_{hg}(z,t),$$

$$\frac{\partial A(z,t)}{\partial z} = -i\frac{\hbar\Omega(t)\check{\rho}_{hg}(z,t)/d + A(z,t)}{2\Delta + i\Gamma}\frac{\Gamma}{2} g n(z),$$

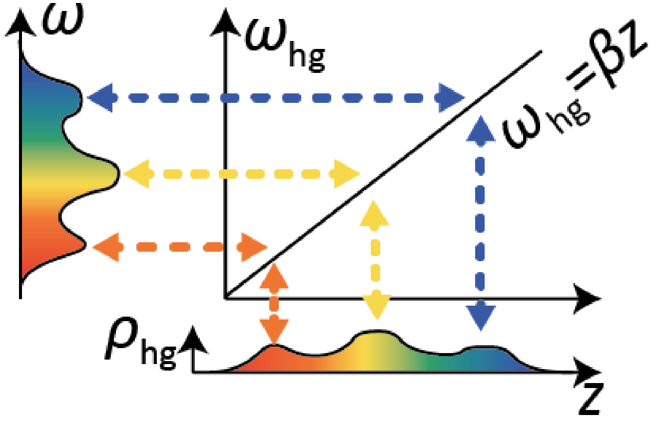

Hosseini et al., Nature 461, 241(2009)

ac-Stark spin-wave phase modulation

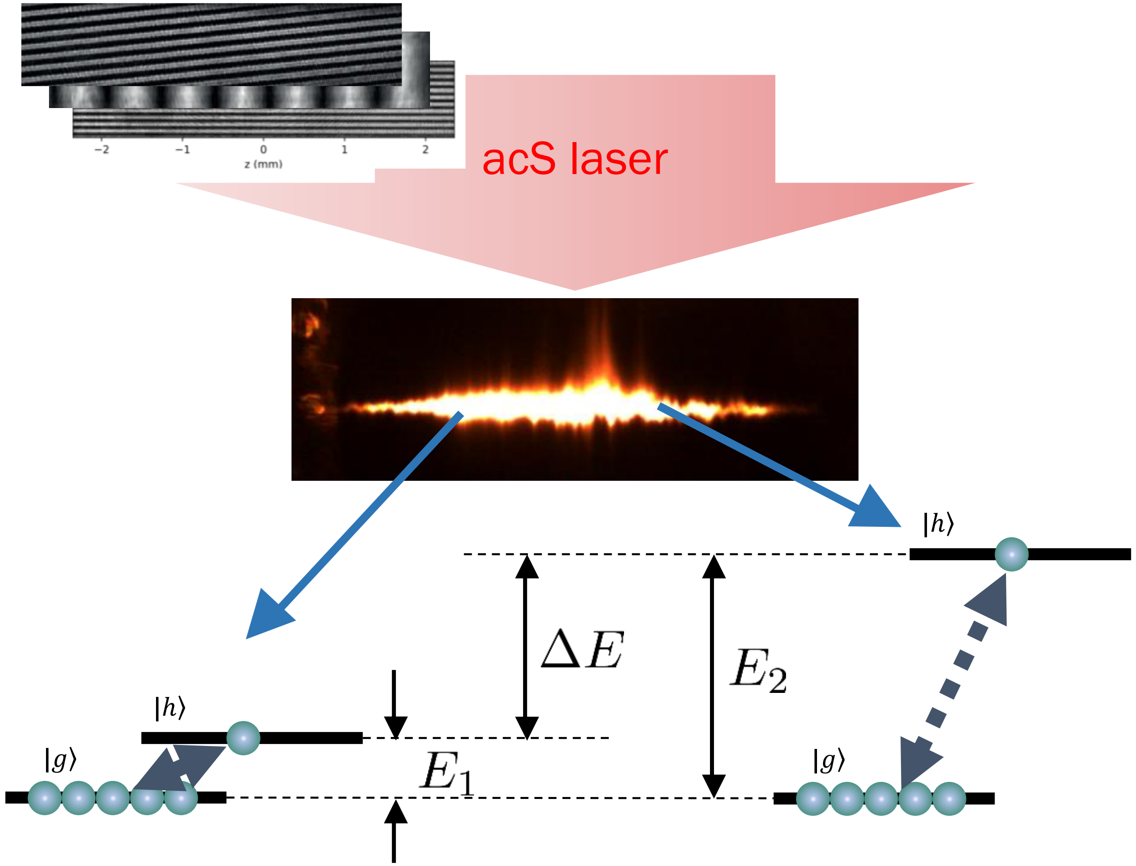

$$\Delta\varphi(y,z) = \Delta E(y,z)T/\hbar$$

Differential phase accumulated during free evolution

Fictitious magnetic fields

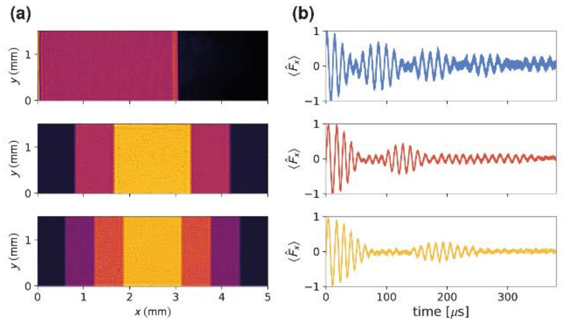

Opt. Lett. 43, 1147 (2018)

Spin-wave Hong-Ou-Mandel interference

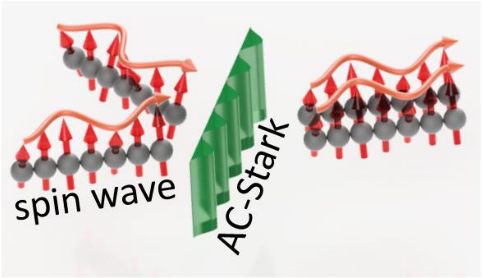

Phys. Rev. Lett. **122**, 063604 (2019)

Spin-wave processor of stored optical pulses

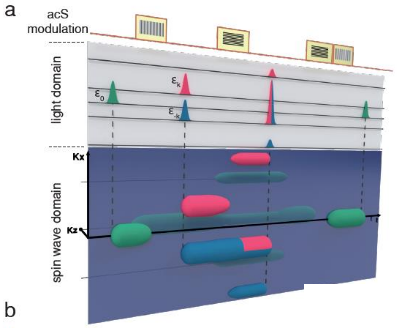

npj Quantum Information **5**, 22 (2019)

Far-field temporal imaging

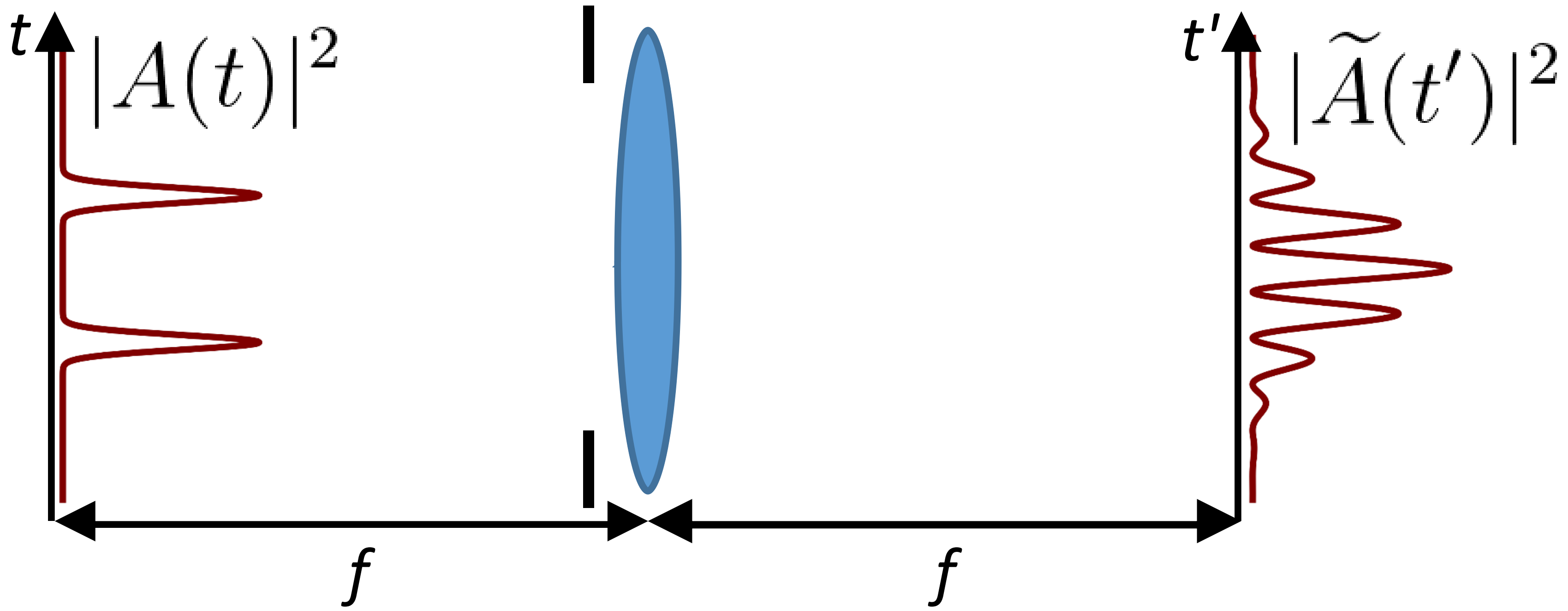

$$|\widetilde{A}(t')|^2 = |\mathcal{F}_t[A(t)](t')|^2$$

Far-field temporal imaging

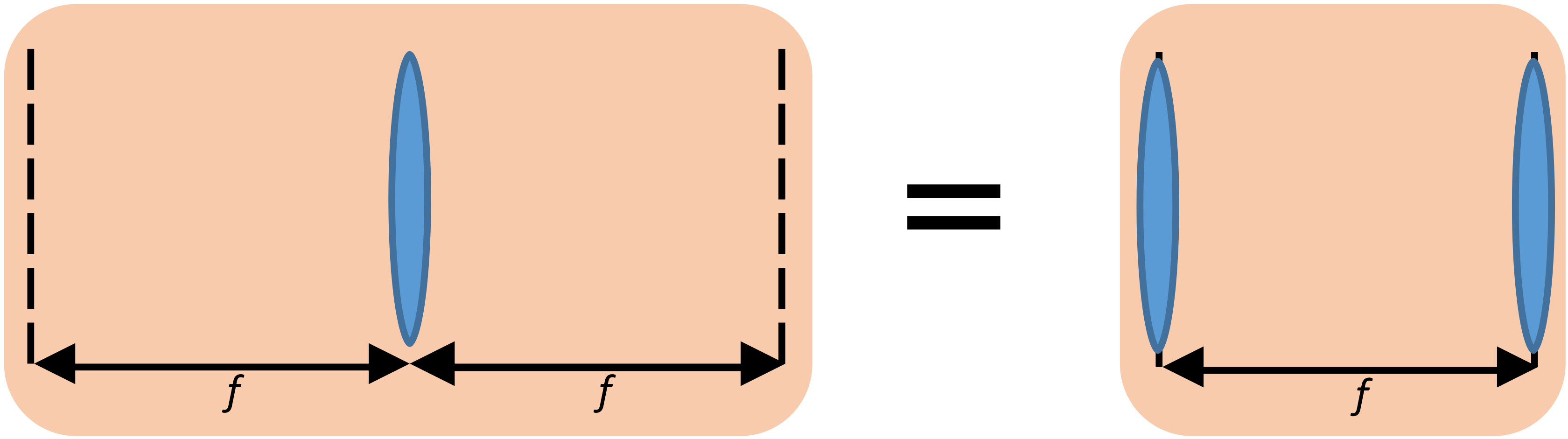

$$\begin{bmatrix} 1 & 0 \\ -\frac{1}{f_t} & 1 \end{bmatrix} \begin{bmatrix} 1 & f_t \\ 0 & 1 \end{bmatrix} \begin{bmatrix} 1 & 0 \\ -\frac{1}{f_t} & 1 \end{bmatrix} = \begin{bmatrix} 0 & f_t \\ -\frac{1}{f_t} & 0 \end{bmatrix} = \begin{bmatrix} 1 & f_t \\ 0 & 1 \end{bmatrix} \begin{bmatrix} 1 & 0 \\ -\frac{1}{f_t} & 1 \end{bmatrix} \begin{bmatrix} 1 & f_t \\ 0 & 1 \end{bmatrix}$$

Time-lens and spectro-spatial mapping

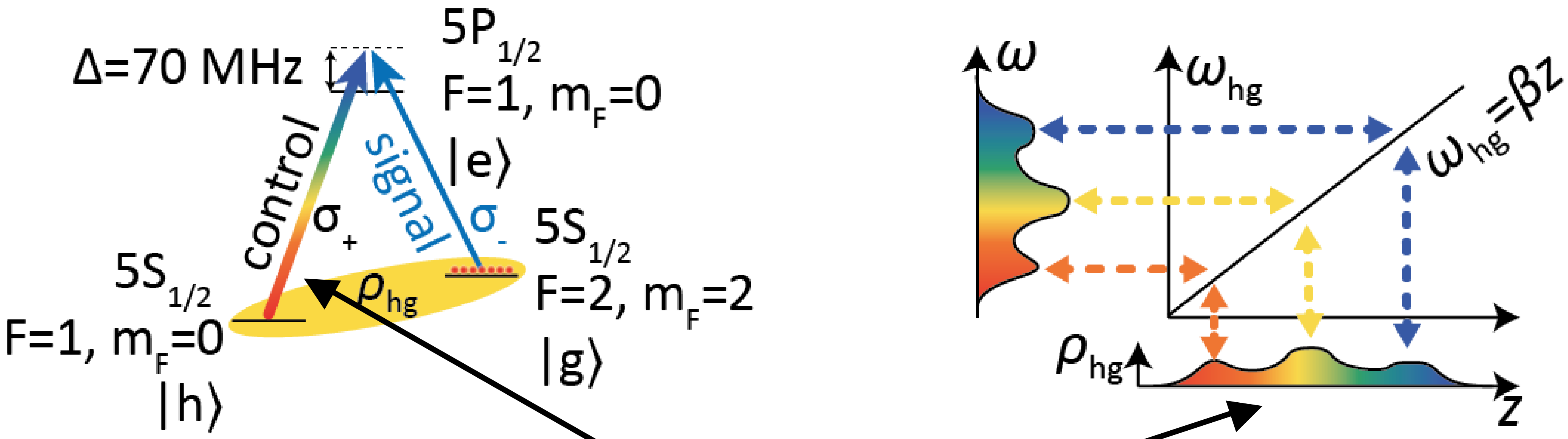

$$\rho_{hg}(z) \propto \widetilde{A}(\beta z)$$

Time-lens realized
by chirped control field

$$\delta\omega(t) = \alpha t$$

$$\begin{bmatrix} 1 & 0 \\ -\frac{1}{f_t} & 1 \end{bmatrix}$$

Temporal propagation

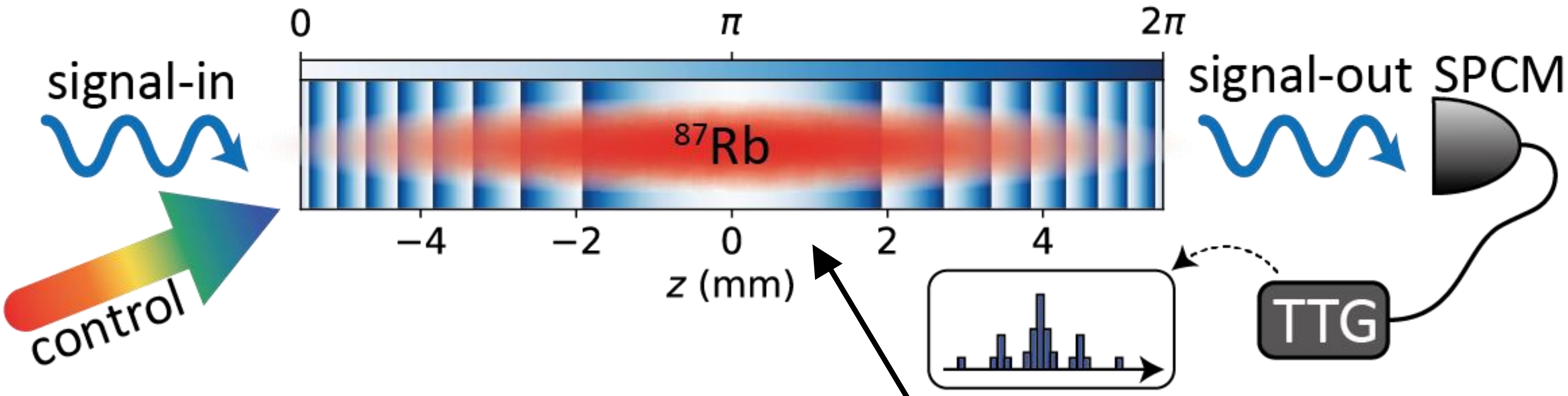

Temporal „free-space" propagation
– a quadratic phase in frequency

$$\tilde{A}(\omega) = \mathcal{F}_t[A(t)](\omega)$$
$$\tilde{A}(\omega) \rightarrow \tilde{A}(\omega)\exp[-i(f_{\mathrm{t}}/\omega_0)\omega^2]$$

Thanks to spectro-spatial mapping the temporal propagation is realized by imposing a quadratic phase (Fresnel) profile onto the atomic coherence ρ_{hg}

Optica 7, 203-208 (2020)

Wigner function transformation

For optical amplitudes: $$\mathcal{W}(t,\omega) = \frac{1}{2\pi}\int \mathcal{A}(t+\xi/2)\mathcal{A}^*(t-\xi/2)\exp(-i\omega\xi)\mathrm{d}\xi$$

For atomic coherence: $$\mathcal{W}(z,k_z) = \frac{1}{\sqrt{2\pi}}\int \varrho_{hg}(z+\xi/2)\varrho^*_{hg}(z-\xi/2)\exp(-ik_z\xi)\mathrm{d}\xi$$

Temporal phase modulations correspond to z-axis reshaping of the atomic coherence Wigner function

$$\mathcal{A}(t) \rightarrow \mathcal{A}(t)\exp\left(i\int\delta(t)\mathrm{d}t\right) \qquad \mathcal{W}(z,k_z) \xrightarrow{\delta(t)} \mathcal{W}(z',k_z)$$

Spectral components of the signal pulse are linked with the complex amplitude of the atomic coherence along the ensemble. At the same time, in time domain, the pulse shape is transferred to wavevector-space components of the coherence.

$$\tilde{\mathcal{A}}(\omega) \leftrightarrow \varrho_{hg}(z)$$

$$\mathcal{A}(t) \leftrightarrow \tilde{\rho}_{hg}(k_z)$$

Real-space phase modulations of the atomic coherence reshape the Wigner function along kz-axis

$$\varrho_{hg}(z) \quad\rightarrow\quad \varrho(z)\exp(i\chi(z)) \qquad \mathcal{W}(z,k_z) \xrightarrow{\chi(z)} \mathcal{W}(z,k'_z)$$

FF-TI (QMTI) - Rotating Wigner function

$$W(t,\omega) = 1/\sqrt{2\pi}\int_{-\infty}^{\infty} A(t+\xi/2)A^*(t-\xi/2)\exp(-i\omega\xi)$$

$$\begin{bmatrix} t' \\ \frac{\omega'}{\omega_0} \end{bmatrix} = \begin{bmatrix} 1 & 0 \\ -\frac{1}{f_t} & 1 \end{bmatrix} \begin{bmatrix} 1 & f_t \\ 0 & 1 \end{bmatrix} \begin{bmatrix} 1 & 0 \\ -\frac{1}{f_t} & 1 \end{bmatrix} \begin{bmatrix} t \\ \frac{\omega}{\omega_0} \end{bmatrix} = \begin{bmatrix} 0 & f_t \\ -\frac{1}{f_t} & 0 \end{bmatrix} \begin{bmatrix} t \\ \frac{\omega}{\omega_0} \end{bmatrix}$$

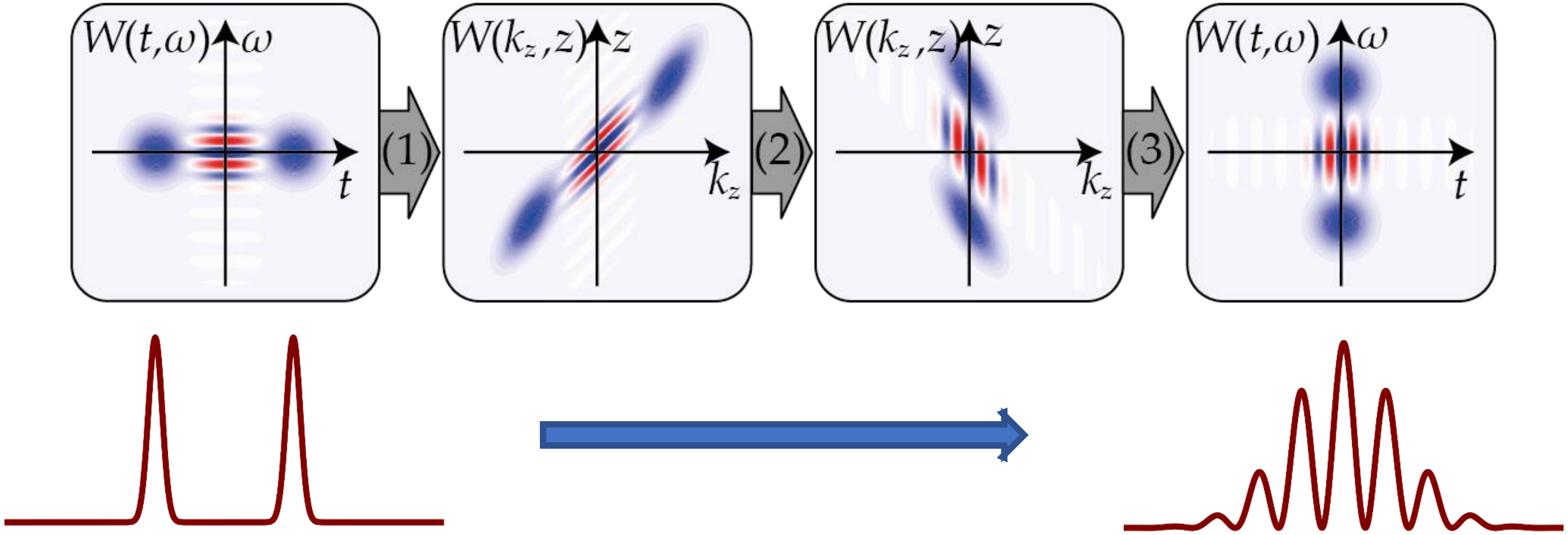

Example input/output

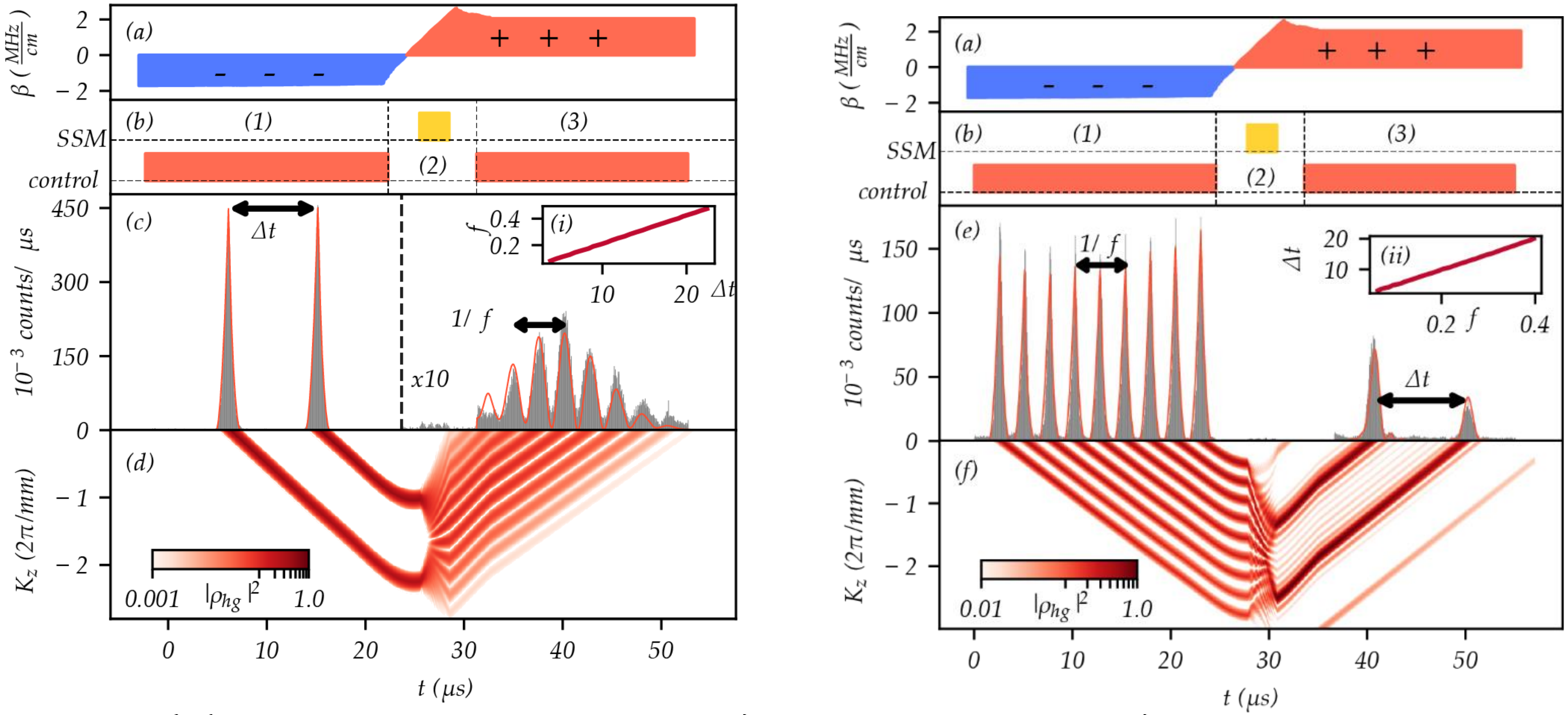

$$\left(\left(\widetilde{A}(\alpha t)\exp(-i(\alpha/2)t^2)\right) * \zeta(\beta t) * \zeta(\beta t)\right)\exp(i(\alpha/2)t^2)$$

Optica 7, 203-208 (2020)

Two incoherent sources

$$\tilde{I}(\omega) = \tfrac{1}{2}\left(|\tilde{\psi}(\omega - \delta\omega/2)|^2 + |\tilde{\psi}_{-}(\omega + \delta\omega/2)|^2\right)$$

$$\tilde{\psi}(\omega) = \tilde{\psi}_{\blacktriangle}(\omega) = \left(\sqrt{2\pi}\sigma\right)^{-1/2} \exp\left(-\frac{\omega^2}{4\sigma^2}\right)$$

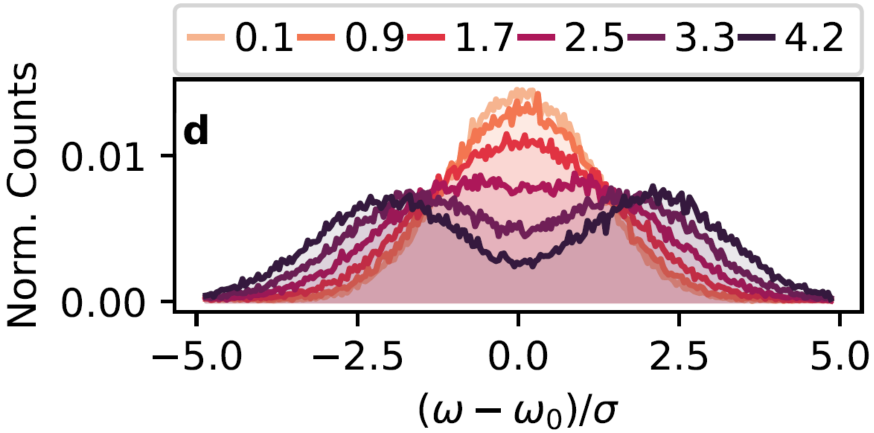

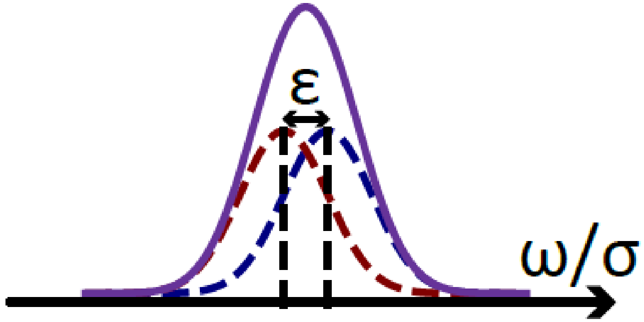

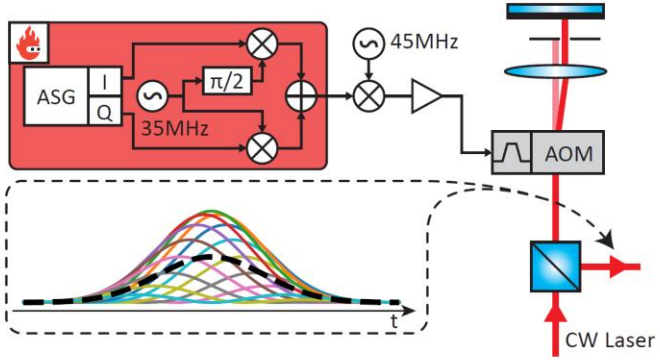

$$\mathcal{S}_{\varphi}(\omega) = \frac{1}{\sqrt{2}}\left(\tilde{\psi}_{\blacktriangle}(\omega - \sigma\varepsilon/2) + e^{i\varphi}\tilde{\psi}_{\blacktriangle}(\omega + \sigma\varepsilon/2)\right)$$

$$\mathcal{W}_{\mathcal{S}}(t,\omega) = \psi_{\blacktriangle}^2(t)(\tilde{\psi}_{\blacktriangle}^2(\omega - \sigma\varepsilon/2) + \tilde{\psi}_{\blacktriangle}^2(\omega + \sigma\varepsilon/2))$$

PuDTAI
Pulse-division time-axis-inversion interferometer

$$1/\sqrt{2}(\mathcal{S}(\omega)+\mathcal{S}(-\omega))$$

$$1/\sqrt{2}(\mathcal{S}(\omega)-\mathcal{S}(-\omega))$$

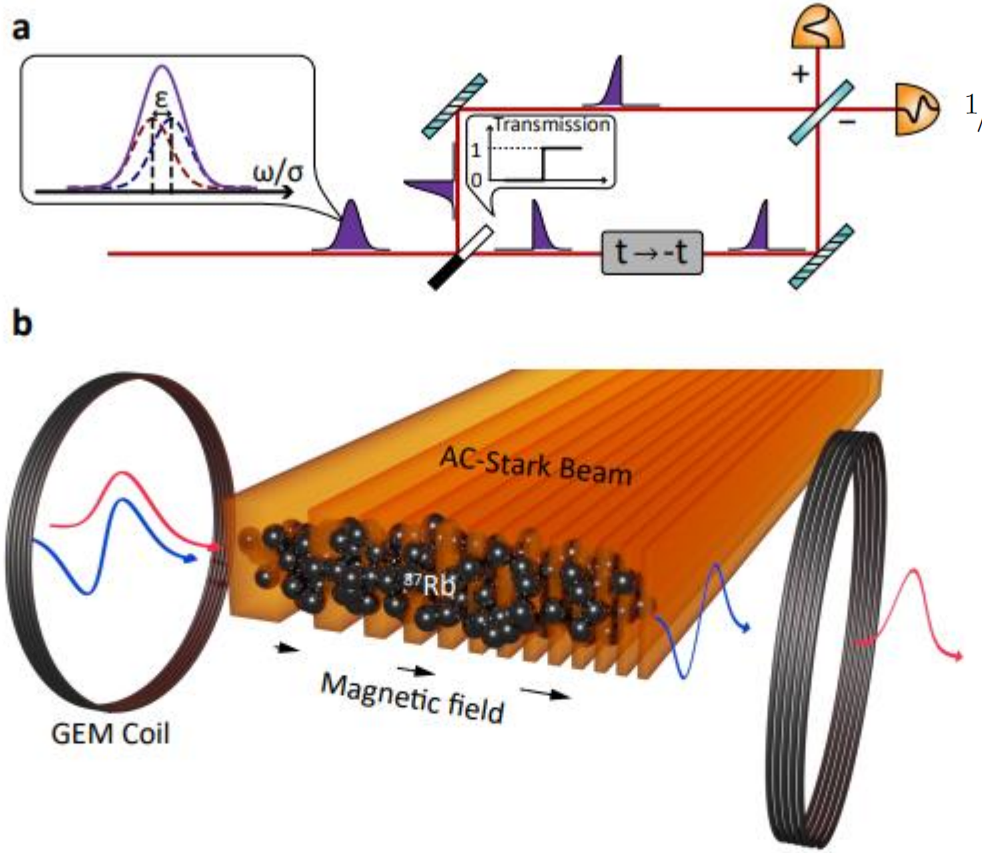

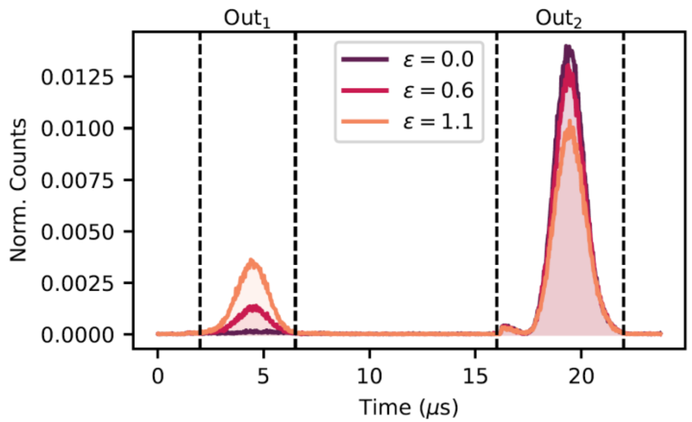

For real space imaging:
Wavefront-division
image-inversion
interferometer

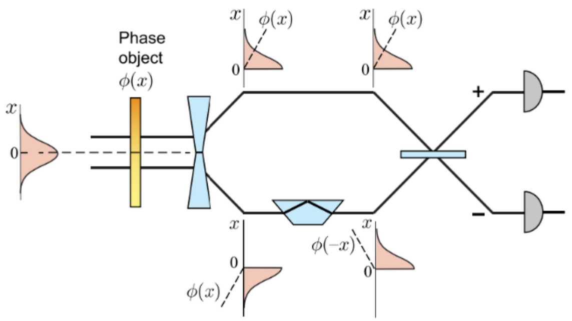

Phys. Rev. A 102, 013712 (2020)

PuDTAI in phase space

$$\mathcal{W}(z,k_z) = \frac{1}{\sqrt{2\pi}} \int \varrho_{hg}(z+\xi/2)\varrho^*_{hg}(z-\xi/2)\exp(-ik_z\xi)\mathrm{d}\xi$$

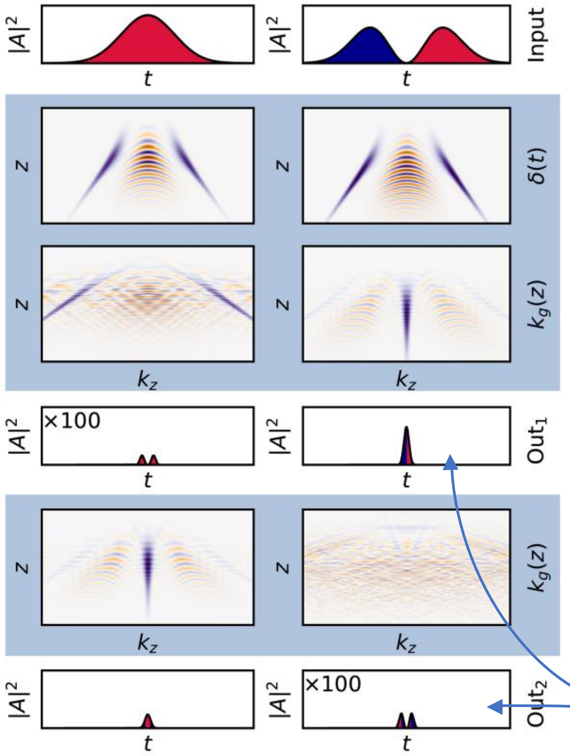

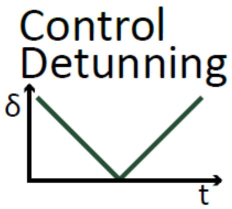

$$\delta(t) = \alpha|t|$$

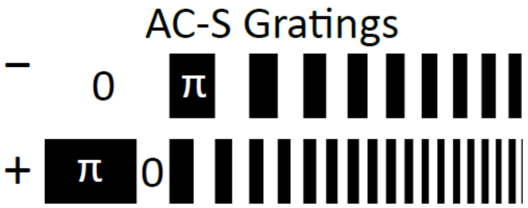

$$k_g = \zeta z \qquad k_g = 2\zeta z$$

The interference happens in the Fourier domain

For the first half of the pulse:

$$\mathcal{A}_-(t) = \begin{cases} \mathcal{A}(t) & t < 0 \\ 0 & t \geq 0 \end{cases}$$

$$k_z \to k'_z = \zeta z$$

$$z \to z' = z - \frac{1}{\zeta} k_z$$

PuDTAI model

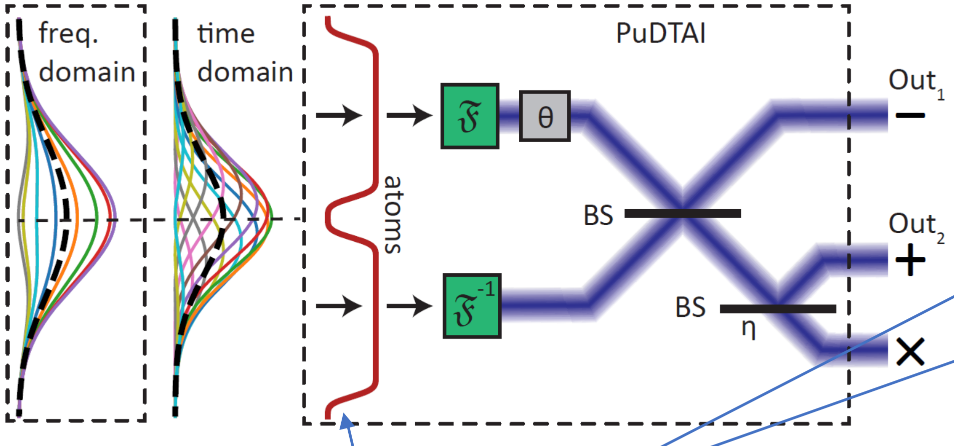

Aperture $\mathfrak{A}$

$$p_1 = \eta_1 \eta_1^{\mathfrak{A}} \frac{1}{2} \left(1 - \mathcal{V}_1 e^{-\frac{\epsilon^2}{8}}\right),$$
$$p_2 = \eta_2 \eta_2^{\mathfrak{A}} \frac{1}{2} \left(1 + \mathcal{V}_2 e^{-\frac{\epsilon^2}{8}}\right),$$
$$p_\times = 1 - p_1 - p_2.$$

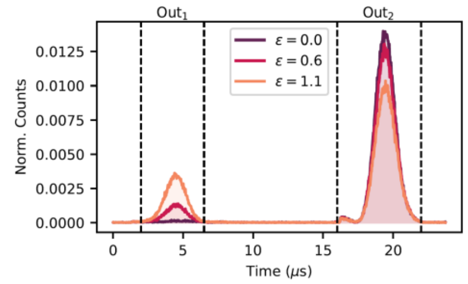

$$\mathcal{F}_{\text{PuDTAI}} = \underbrace{\eta_1 \eta_1^{\mathfrak{A}} \frac{e^{-\frac{\varepsilon^2}{8}} \varepsilon^2 \mathcal{V}_1^2}{32 e^{\frac{\varepsilon^2}{8}} - 32 \mathcal{V}_1}}_{\mathcal{F}_1} + \underbrace{\eta_1 \eta_2^{\mathfrak{A}} \frac{e^{-\frac{\varepsilon^2}{8}} \varepsilon^2 \mathcal{V}_2^2}{32 \left(e^{\frac{\varepsilon^2}{8}} + \mathcal{V}_2\right)}}_{\mathcal{F}_2},$$

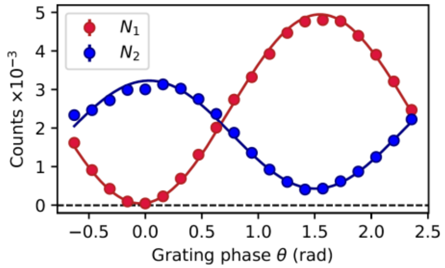

The aperture results in losses but mostly in the symmetric port.
For "hard" aperture:

$$\eta_1^{\mathfrak{A}} \approx \text{erfc}\left(\frac{\omega_{\mathfrak{A}}}{\sigma}\right) + \frac{\omega_{\mathfrak{A}}}{\sigma} \exp\left(-\frac{\omega_{\mathfrak{A}}^2}{2\sigma^2}\right) \sqrt{\frac{2}{\pi}}$$
$$\eta_2^{\mathfrak{A}} \approx \text{erfc}\left(\frac{\omega_{\mathfrak{A}}}{\sigma}\right)$$

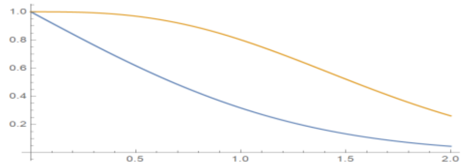

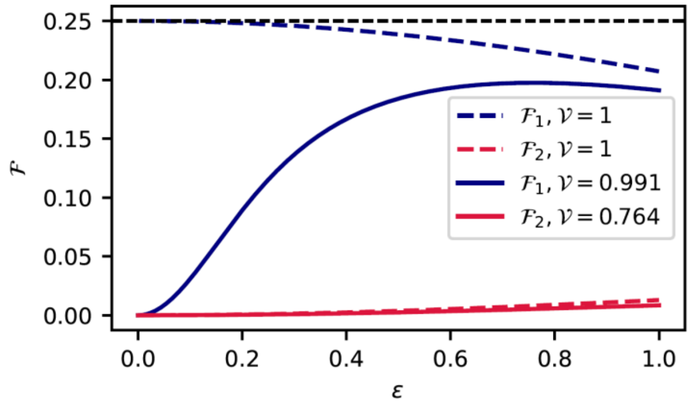

For small separations the information is concentrated in the anti-symmetric port

Fisher information density at SLIVER (PuDTAI) outputs

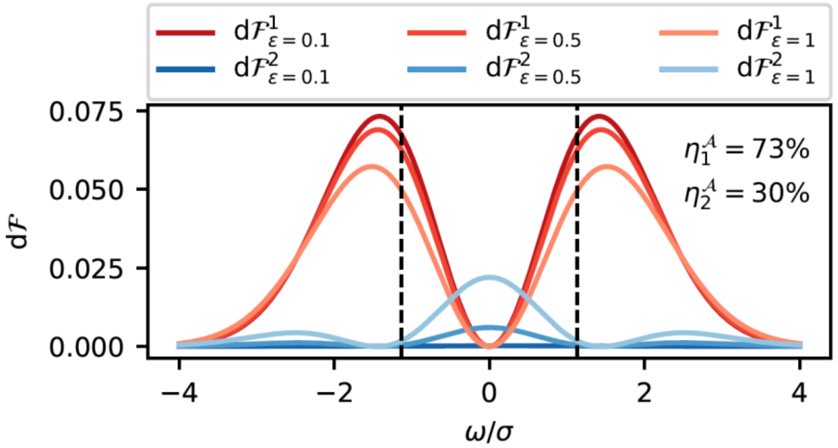

$$\mathrm{d}\mathcal{F}_i = \frac{1}{p_i(\omega)} \left(\frac{\partial}{\partial \varepsilon} p_i(\omega) \right)^2 \mathrm{d}\omega$$

$$\mathcal{F}_i = \int_{\mathfrak{A}} \mathrm{d}\mathcal{F}_i$$

The FI is concentrated in the lobes, thus removal of the center part is acceptable

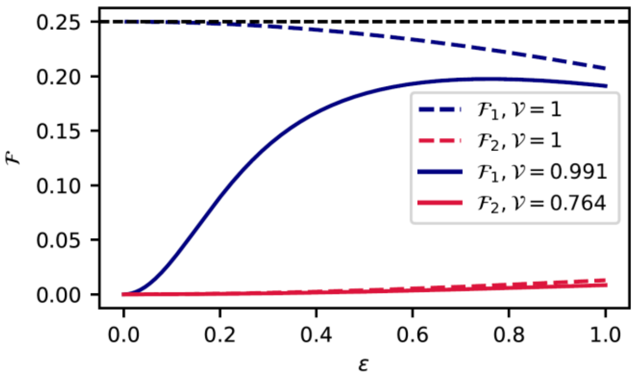

The symmetric port serves only as a source brightness reference and for small separations contains no information arXiv:2106.04450

Separation estimation

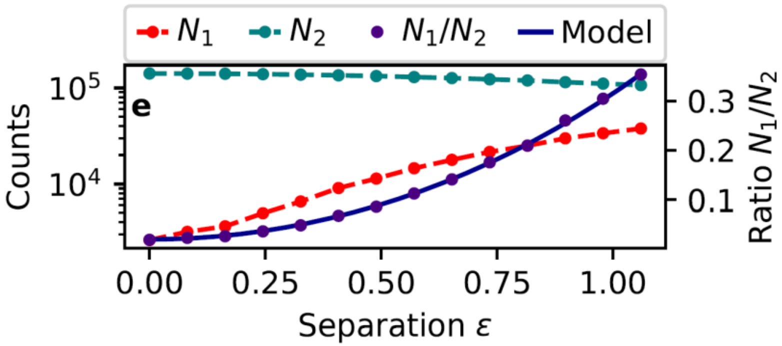

$$p_1 = \eta_1 \eta_1^{\mathfrak{A}} \frac{1}{2}\left(1 - \mathcal{V}_1 e^{-\frac{\epsilon^2}{8}}\right) \rightarrow N_1$$

$$p_2 = \eta_2 \eta_2^{\mathfrak{A}} \frac{1}{2}\left(1 + \mathcal{V}_2 e^{-\frac{\epsilon^2}{8}}\right) \rightarrow N_2$$

$$\rightarrow \hat{\varepsilon}(N_1/N_2)$$

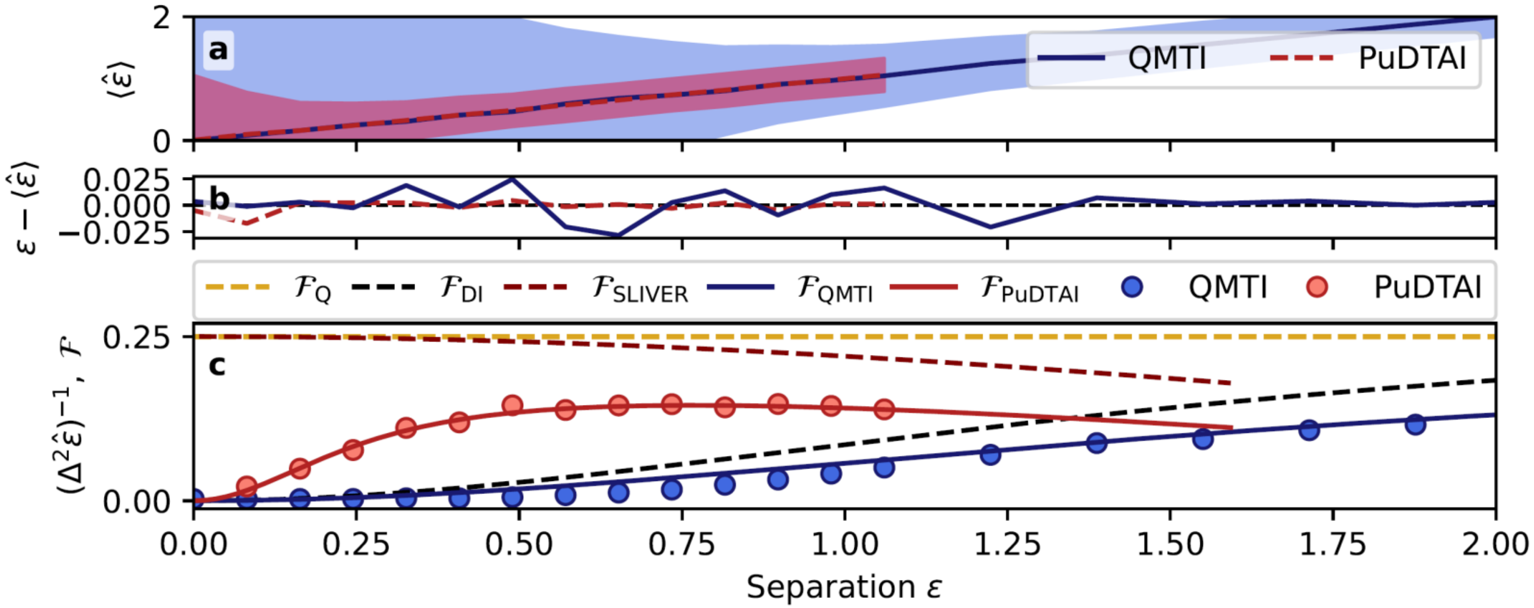

Maximum likelihood estimation in both cases

QMTI raw data:

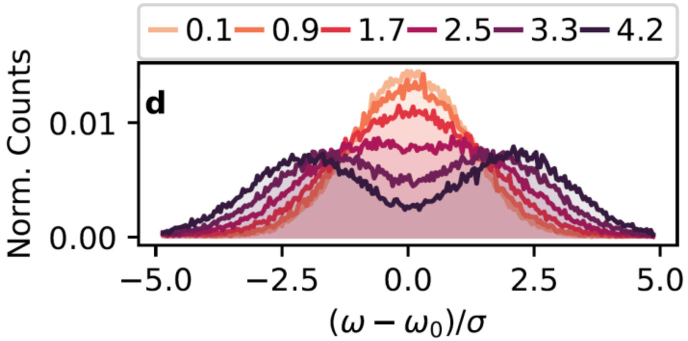

Comparison

Our approach: PuDTAI

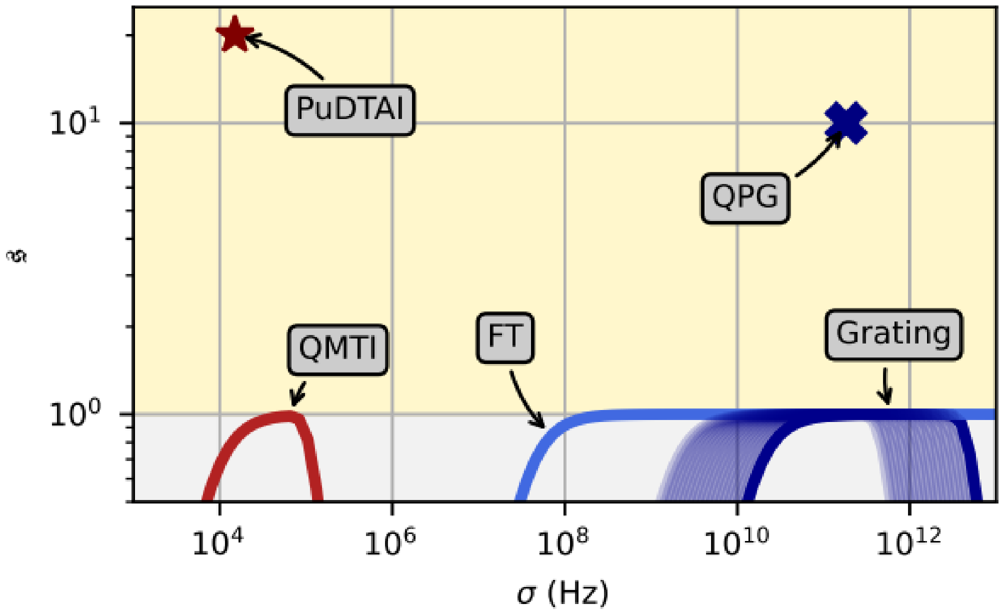

Superresolution parameter:

$$\mathfrak{s} = \lim_{\varepsilon \to 0} (\mathcal{F}/\mathcal{F}_{\mathrm{DI}})$$

See also: [Phys. Rev. Applied **15**, 034071]

Quantum Pulse Gate (QPG) - SPADE

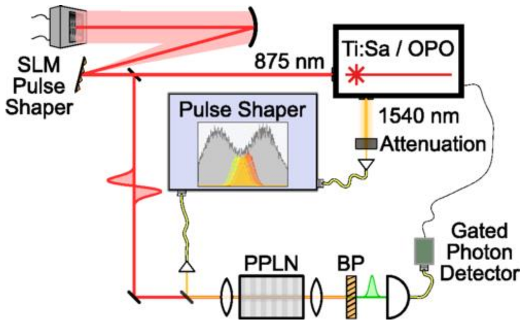

Phys. Rev. Lett. 121, 090501 (2018)

Homodyne/Heterodyne (under development)

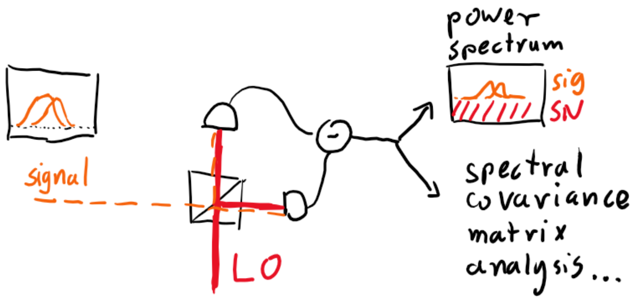

Phys. Rev. A 102, 063526 (2020)

Acknowledgments

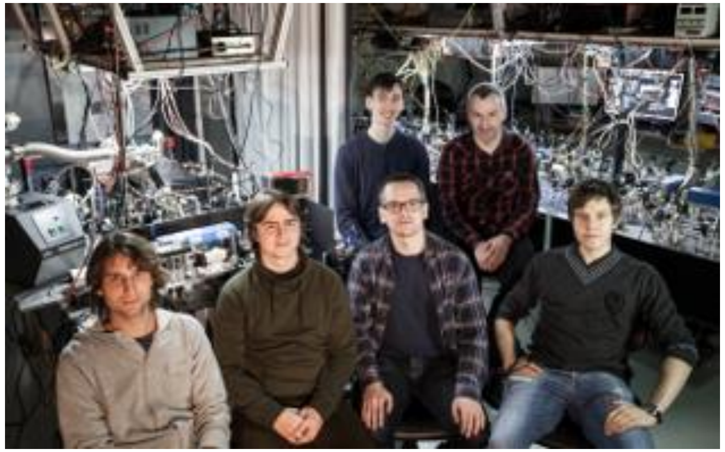

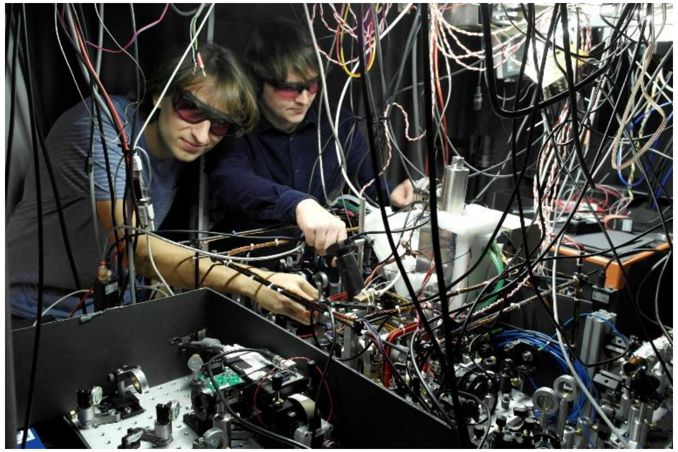

Joint work with:
Mateusz Mazelanik
Adam Leszczyński

We acknowledge insightful discussions with:
Wojciech Wasilewski
Konrad Banaszek
Rafał Demkowicz-Dobrzański
Marcin Jarzyna
Stanisław Kurdziałek

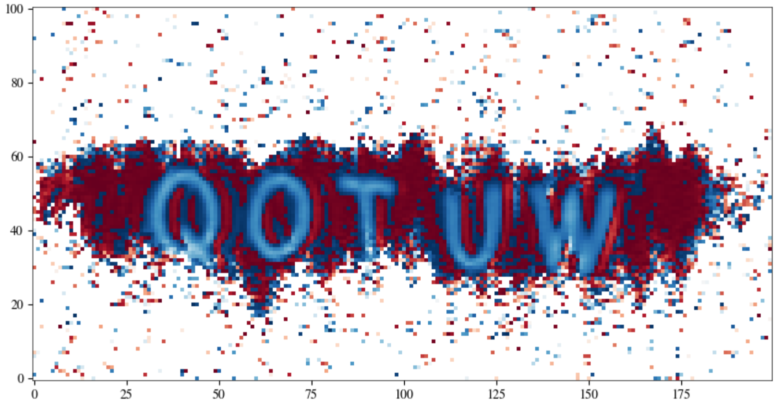

Office of Naval Research
USN
ONR
Science & Technology

Diamentowy Grant

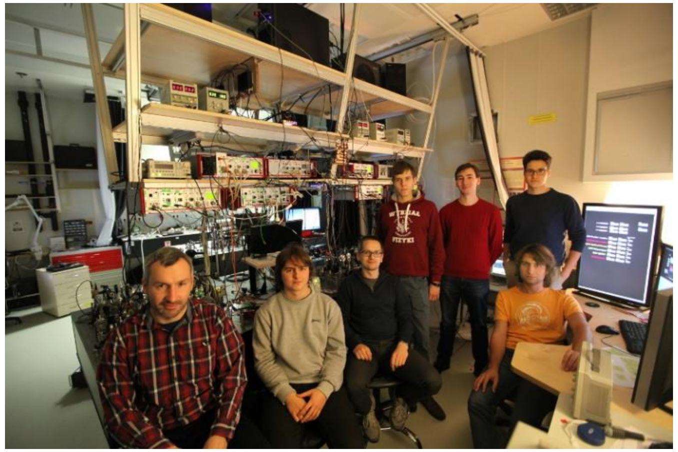

[Centre for Quantum Optical Technologies (QOT)]

European Funds Smart Growth
Republic of Poland
FNP Foundation for Polish Science
European Union European Regional Development Fund
National Science Centre Poland